2006

EM Algorithm for Multiple Wideband Source Localization

Kiran Kumar Mada
Louisiana State University and Agricultural and Mechanical College

EM ALGORITHM FOR MULTIPLE WIDEBAND SOURCE LOCALIZATION

A Thesis

Submitted to the Graduate Faculty of the
Louisiana State University and
Agricultural and Mechanical College
in partial fulfillment of the
requirements for the degree of
Master of Science in Electrical Engineering

in
The Department of Electrical and Computer Engineering

by
Kiran Kumar Mada
Bachelor of Engineering, Osmania University, 2003
August 2006

Acknowledgements

I would like to acknowledge certain people who have encouraged, supported and helped me complete my thesis at LSU.

I am extremely grateful to my advisor Dr.Hsiao-Chun Wu for his guidance, patience and understanding all through this work. His suggestions, discussions and constant encouragement have helped me gain a deep insight in the field of signal Processing. I would like to thank Dr. Subhash Kak and Dr. Suresh Rai for sparing their time to be a part of my advisory committee. I would also thank Sameer Hereleker and Ms.Huang for all their help. I am grateful to my parents Mr.and Mrs. Sudhakar Reddy for the tremendous amount of inspiration they have given me.

I would like to thank all my friends here at LSU, who have helped me all through my stay at LSU and have made my stay a pleasant one.

Table of Contents

List of Figures

Abstract

A computationally efficient algorithm using the expectation-maximization (EM) algorithm for multiple wideband source localization in the near field of a sensor array/area is addressed in this thesis. Our idea is to decompose the observed sensor data, which is a superimposition of multiple sources, into the individual components in the frequency domain and then estimate the corresponding location parameters associated with each component separately. Instead of the conventional alternating projection (AP) method, we propose to adopt the EM algorithm in this work; our new method involves two steps, namely Expectation (E-step) and Maximization (M-step). In the E-step, the individual incident source waveforms are estimated. Then, in the M-step, the maximum likelihood estimates of the source location parameters are obtained. These two steps are executed iteratively and alternatively until the pre-defined convergence is reached. The computational complexity comparison between our proposed EM algorithm and the existing AP scheme is investigated. It is shown through Monte Carlo simulations that the computational complexity of the proposed EM algorithm is significantly lower than that of the existing AP algorithm.

Chapter 1 Introduction to Source Localization

1.1 Introduction

Source localization has long been intriguing for signal processing researchers due to the corresponding broad applications in the field of radar, sonar, geophysics, wireless communications and acoustic tracking etc,. Nowadays, many endeavors are still dedicated to the new source localization problems emerging from the stringent requirement for both superior performance and cost-effective implementation. Generally speaking, source localization refers to the estimation of the spatial coordinates for the moving sources and their paths. Existing techniques have been employed for the estimation of direction-of-arrival (DOA), which is a simplified source localization problem, for narrowband sources in the far field [1-5]. On the other hand, there has been growing interest in locating wide-band source signals in the near field recently, which involves both range and direction of arrival (DOA) estimation. In this thesis work, we focus on the localization of acoustic sources close to the microwave sensor array.

Array processing for wideband signals can be applied for many practices such as sonar, microphone array for teleconferencing, spread spectrum communications, etc. Extensive literature on the wide-band source localization or DOA estimation can be found in [6-11]. The frequency spectrum of a wide-band signal occupies a broad bandwidth. Hence, the signal processing algorithms have to be modified to accommodate this characteristic. For the wide-band source localization, the recorded data at each sensor is partitioned into non-overlapping frames or *snapshots*. Then the discrete Fourier transform (DFT) is applied for each snapshot to generate the short-time frequency

spectra. Consequently, in every frequency bin, it is converted to a traditional narrow-band source localization problem.

There exist some wide-band source localization techniques. In the incoherent signal-subspace method (ISM) [12], each frequency bin is processed individually and the outcomes are combined to estimate the DOA. However, the application of the ISM for coherent (correlated) signals is not promising. An alternative to the ISM is the coherent signal subspace method (CSM) [13]. In the CSM, the correlation matrices at different frequency bins are combined and incorporated with the pre-estimation of the DOAs to form a "universal" correlation matrix, which is a sufficient statistics for the observation vectors [14]; a high-resolution algorithm, such as MUSIC [15], has been applied to this sufficient statistics to estimate the DOAs thereupon; the combination of narrow-band signals is performed using the linear transformation of the observation vectors and this technique is called *focusing*. The focusing operator is characterized as a matrix which performs the singular-value decomposition to extract the principal components in the frequency domain. The CSM can resolve the coherent source localization problem and has higher detection accuracy than the ISM [13]. However, the drawback of the CSM is the additional requirement for a preprocessor; it needs to construct the focusing matrices. Moreover, the CSM techniques have never been tested for the near-field case.

Another potential solution to the wideband source localization problem is the time-delay estimation method, which is also called least-square (LS) method. The LS method involves two steps. In the first step, the relative time delays, or the signal arrival time difference between any pair of sensors, are estimated and then the source locations are determined in the second step from the relative time delays accordingly. Possible close-form solutions for the second step in the LS method have been discussed in [16-19],

which are based on the spherical interpolation, hyperbolic intersection, and linear integration, respectively. However, the LS method cannot distinguish the multiple sources individually.

For the wide-band source localization in the near field, the maximum-likelihood (ML) method has been regarded as the optimal approach and it is robust for coherent source signals [6]. Nevertheless, once there exist multiple sources, the ML scheme leads to a nonlinear optimization problem which requires a heavy computational burden and thus makes the ML algorithm less attractive especially in the energy-constrained sensor networks. In reality, the sources need to be located at the senor nodes without the possible aid of the external computational resource. Since energy is strictly limited for the low-cost sensors, it is very important to reduce the computational complexity involved in any algorithm. Hence, it has been challenging for researchers to design the algorithms which can be implemented in real time. In this thesis, we propose the expectation maximization (EM) algorithm to achieve the numerical ML maximization and it is rather computationally efficient compared to the alternating projection (AP) method in [6, 20].

Felder and Weinstein proposed the generic EM algorithm in [21] to estimate the parameters associated with the superimposed signals and extended it to search for the signal parameters in the ML sense for the array signal processing in [22]. EM based techniques have also been applied for the parameter estimation of superimposed signals and the multi-sensor signal enhancement in [23, 24]. The recursive EM and SAGE methods were developed in [25] for unknown model orders. In addition, EM-based narrow-band source localization algorithms can also be found in [26-28]. In this thesis work, we modify the EM algorithm, for the general multiple source localization problem, when the wide-band sources are present in the near field, which evolves from the DOA

estimation method for the narrow-band sources in the far field in [5]. If the wide-band sources are considered, the source signal signature or characteristics is unavailable at the sensor array and the method in [5] cannot be applied. Therefore, in this thesis, we use the discrete-Fourier transform (DFT) filter bank to decompose the wide-band signals collected by the sensors and then estimate the complete set of parameters such as source waveforms and source locations.

1.2 Thesis Outline

The thesis is organized as follows. In Chapter 2, we provide the introduction to wave propagation, sensor network, and source characteristics; then we discuss the mathematical model which is adopted in this thesis; finally we address the existing wideband source localization algorithms as well as their advantages and disadvantages. Chapter 3 paves the foundation for the frequency analysis of the wide-band signals; we introduce the discrete Fourier transform to decompose the wide-band signal time-series into the spectra in the frequency domain. In Chapter 4, first we discuss the basic EM algorithm for the maximum-likelihood estimation of the underlying parameters; then, we derive the EM algorithm for multiple wideband source localization in near field. To test the effectiveness of our proposed method, we carry our simulations and present the simulation results in Chapter 5; we also compare the computational complexity of our proposed EM algorithm with that of the AP algorithm in [6]. Concluding remarks will be drawn in Chapter 6.

Chapter 2 Fundamentals of Source Localization and Existing Algorithms

Source localization using sensor arrays has been exploited for decades [1]. The purpose of this chapter is to introduce different source localization algorithms and discuss the corresponding applications and challenges for the wideband source localization. Following will be focused on wave propagation, signal modeling at the sensor nodes and sensor network.

2.1 Wave Propagation

Wave propagation properties are very important in dealing with the sensor data since it characterizes the relative positions of the sources to the sensor array. Wave can be defined as the transfer of energy (or) the disturbance from one point to another between two points. A typical wave is illustrated in Fig. 2.1. Consider a wave with propagation speed *C*, wave length λ, and frequency *f*. Then, the relationship among the above-mentioned parameters can be given by

$$\lambda = \frac{C}{f}. \tag{2.1}$$

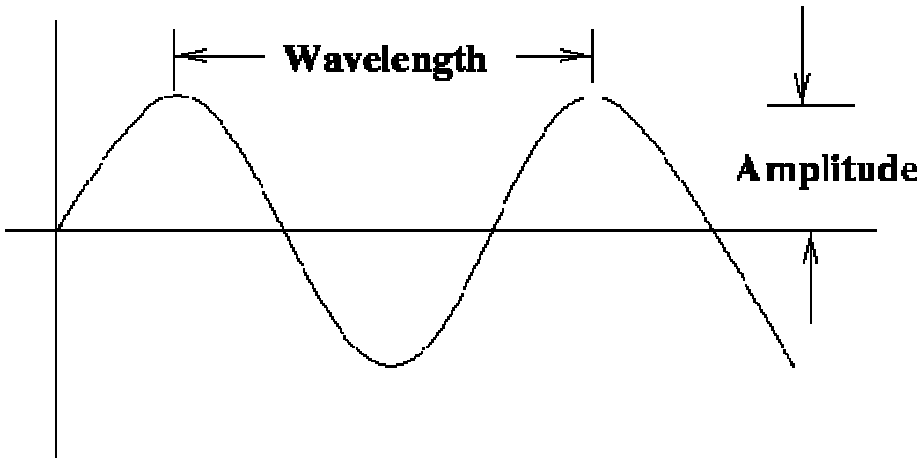

Figure 2.1 A simple wave.

Now, let us consider an acoustic wave which is generated by a vehicle in movement. Thus, the originated wave emitted from the source (vehicle) will travel in all directions. If the propagating medium (air for example) is isotropic, the traveling wave will propagate at a uniform speed in all directions as shown in Fig. 2.2.

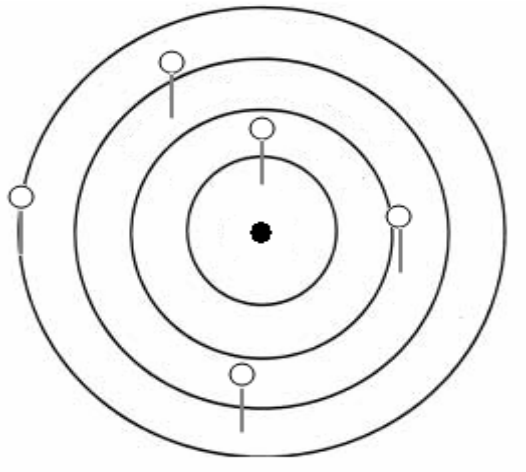

Figure 2.2 Propagation of a wave in an isotropic medium emitted from the point source (reaching sensors).

For coping with the source localization in the near field, the shapes of the wave fronts reaching the sensor nodes play a major role in determining the corresponding signal gains at the sensor nodes. Wave front is an imaginary line representing all in-phase parts of a traveling wave with an identical wavelength from the source. The wave front shape depends on the nature of the source; a point source will emit the waves having circular or spherical wave fronts as shown in Fig. 2.2, while a large extended source will emit the waves whose wave fronts are relatively flat as a plane.

In this thesis, we consider the near-field case and hence the wave front from a point source reaching the sensor nodes is circular accordingly as shown in Fig. 2.2. There fore, the signal gains at the sensor nodes depend on the distances between sources and the

sensors, whereas in the far-field case, it can be modeled as many point sources close to each other in a straight line and they give rise to the plane waves as shown in Fig. 2.3.

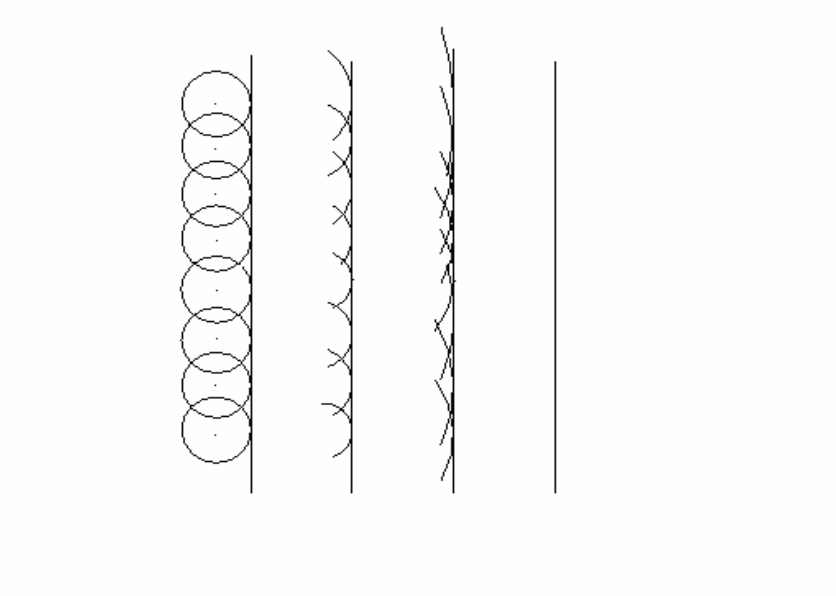

Figure 2.3 Plane waves formed by many point sources closely gathered.

2.2 Sensor Network

Wireless sensor networks are one of the popular contemporary research topics. Advances in the hardware technology enable low-cost, low-power, miniature sensors for the applications in remote-sensing, detection, classification, localization and tracking. A sensor network is an array of sensors which can be interconnected via the communication network as shown in Fig. 2.4. The data acquired at the sensor nodes is shared among the sensors and the distributed computing system (personal computer). This distributed computing system estimates and extracts the relevant and useful information from the acquired sensor data. The sensors are battery-powered and have limited wireless communication bandwidth. Therefore, efficient, reliable and less complicated source localization algorithms are needed for the practical sensor networks.

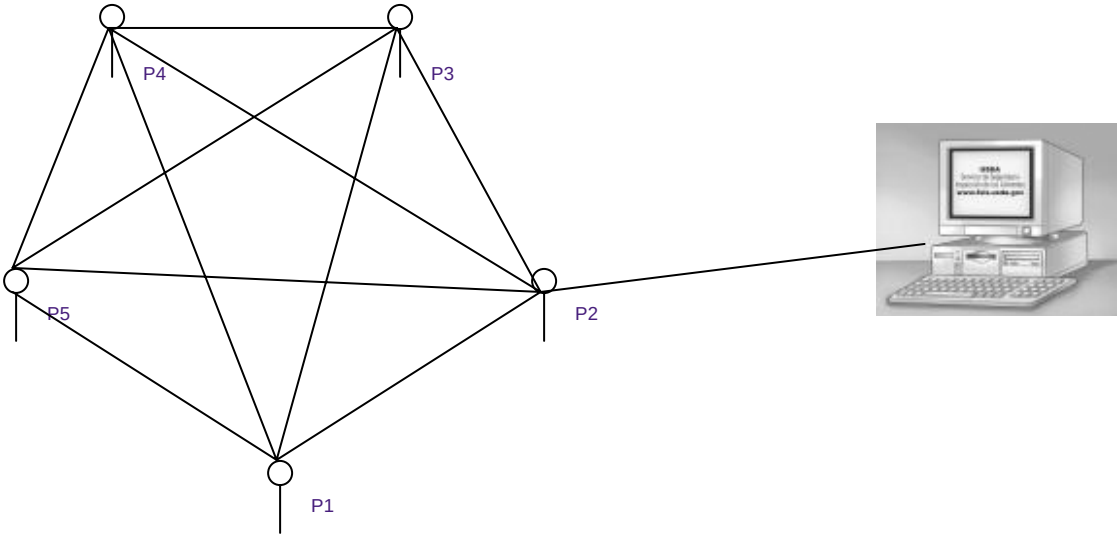

Figure 2.4 Sensor network connected with a personal computer (P1, P2, …, P5 represent sensors).

2.3 Classification of Source Localization Problems for Wireless Sensor Networks

As stated in the previous subsection, sensor nodes collect the signals originating from the sources. This sensor data depend on the physical features associated with the sources, which can be listed in the following table.

In this thesis, we will deal with the acoustic sources. In practice, the movements of personnel, car, truck, wheeled vehicle, and vibrating machinery can generate acoustic signals. These acoustic signals are considered wideband since the corresponding ratios between the high frequency components and the low frequency components are very high (in the orders of 100-500) [29]. For comparison, the radio-frequency (RF) waveforms in the wireless telecommunications have the corresponding ratios in the orders of 1-1.03 only. Thus, the RF signals are referred to as narrowband signals accordingly.

Table 2.1. Characterization of source signals (Note: * denotes the underlying features considered in this thesis).

Source Modality	Acoustic*, Seismic
Signal Bandwidth	Narrow-band, Wide-band*
Propagation Medium	Free-space*, Reverberant space
Signal Propagation Distance	Near-field*, Far-field
Number of sources	Single source, Multiple sources*

Let's consider the location of a source relative to a sensor now. When a source is placed close to the sensor array, the signal wave-front received at the sensor node is curved, i.e., the signal gain at the sensor node, which is inversely proportional to the squared distance between the source and the sensor, is distinct at different sensors. This is the particular scenario for the near-field case. In the far-field case, the wave-front approaching the sensor array is a plane that gives rise to the uniform signal gains at the all sensor nodes. This far-field scenario arises when the source is very far away from the sensor array.

Another crucial factor to be concerned is the propagation speed. The speed of propagation depends on the medium through which the signal travels. For an acoustic source, the propagation speed in the air is approximately 345 meter/second. The speed of propagation also depends on the wind velocity and the temperature of atmosphere. The turbulent and windy atmospheric conditions could also affect the coherency of the acoustic signal wave-fronts and thus degrade the coherent processing of the signals. For simplicity, here we consider the atmosphere to be free of turbulence.

The received signal energy at the sensor node also depends on the aforementioned atmospheric conditions. The signal energy up to 10-90% can be lost when the traveling waves strike the walls or different objects indoors. Even in the free fields outdoors, the signal energy loss can occur due to the signal reverberations from the walls, hills, and some large objects. In this thesis, we consider that the data is acquired in the free-space environment and thus the only factor which affects the received signal energy is the squared distance between the sensor and the source.

2.4 Sensor Signal Model

Consider a randomly distributed sensor array of *P* sensors, which collect data from *M* sources. Let the signal generated by the source *m* located at $\underline{r_s}^{(m)}$, be $s_0^{(m)}(t)$ at a time instant *t*. Then the received signal at the p^{th} sensor located at $\underline{r_p}$, is $s_0^{(m)}(t - T_p^{(m)})$, where $T_p^{(m)}$ is the propagation delay from the m^{th} source to the p^{th} sensor. The aforementioned notations are suitable for the far-field case, since it is assumed that point sources emit signals in an isotropic medium and it gives rise to a spherical traveling wave-front whose amplitude is inversely proportional to the distance between the sensor and the source. All points lying on the surface of a sphere with radius *R* will then share a common phase and they constitute a *wave-front*. The distances between the sources and the receiving sensors determine whether the wave sphericity should be taken into account or not. Since we consider the near-field case here, the wave-fronts received at the sensors are spherical. Then the p^{th} sensor's received signal due to the m^{th} source signal is $a_p^{(m)} s_0^{(m)}(t - T_p^{(m)})$, where $a_p^{(m)}$ is the signal gain of the m^{th} source at the p^{th} sensor (inversely proportional to the squared distance between the source and the sensor). Now,

the data collected by the p^{th} sensor at time n, which is a superimposition of all sources, can be formulated as

$$x_p(n) = \sum_{m=1}^{M} a_p^{(m)} s_0^{(m)}\left(n - t_p^{(m)}\right) + w_p(n), \text{ for } n = 0,1,\cdots,L-1,\ p = 1,\cdots,P, \qquad (2.2)$$

where

$a_p^{(m)}$ is the signal gain corresponding to the m^{th} source at the p^{th} sensor, $m = 1,\cdots,M$;

$s_0^{(m)}$ denotes the m^{th} source signal waveform;

$t_p^{(m)}$ is the propagation delay in samples from the m^{th} source to the p^{th} sensor;

$w_p(n)$ represents the zero-mean independently identically distributed Gaussian noise process with variance σ^2. Several location parameters can be specified as follows:

$$t_p^{(m)} = \left\| \underline{r_s}^{(m)} - \underline{r_p} \right\| / v \text{ (propagation delay),}$$

$\underline{r_s}^{(m)} \in \mathsf{R}^{2\times 1}$: the m^{th} source location,

$\underline{r_p}$: the p^{th} sensor location,

v: the speed of propagation in meters/sec.

Taking the DFT for both sides of Eq. (2.2), we have

$$\underline{X}(k) = \overline{D}(k)\,\underline{S_0}(k) + \underline{U}(k),\ k = 0,1,\cdots,N-1, \qquad (2.3)$$

where

$\underline{X}(k) \equiv \left[X_1(k) \quad \cdots \quad X_P(k)\right]^T \in \mathsf{C}^{P\times 1}$ ($X_p(k)$ is the k^{th} DFT point of $x_p(n)$, $p = 1,\cdots,P$);

$\overline{D}(k) \equiv \left[\underline{d}^{(1)}(k) \quad \cdots \quad \underline{d}^{(M)}(k)\right] \in \mathsf{C}^{P\times M}$ consists of M steering vectors, each given by

$$\underline{d}^{(m)}(k) \equiv \left[d_1^{(m)}(k) \quad \cdots \quad d_P^{(m)}(k) \right]^T \in \mathbb{C}^{P\times 1}$$

and

$$d_p^{(m)} \equiv a_p^{(m)} e^{-j2\pi t_p^{(m)}/N};$$

$$\underline{S_0}(k) \equiv \left[S_0^{(1)}(k) \quad \cdots \quad S_0^{(M)}(k) \right]^T \in \mathbb{C}^{M\times 1}$$ ($S_0^{(m)}(k)$ is the k^{th} DFT point of $s_0^{(m)}$, $m = 1, \cdots, M$).

The source signal spectra $\underline{S_0}(k)$ are unknown and deterministic. The noise spectral vector $\underline{U}(k) \in \mathbb{C}^{P\times 1}$ is a complex-valued zero-mean white Gaussian process and each element has a variance $L\sigma^2$.

2.5 Existing Methods for Wide-band Source Localization

Several methods have been proposed for the wide-band source localization [6-11]. Among them, we will discuss three major approaches in this chapter, namely *coherent signal subspace method* (CSM), *time–delay estimation* or *LS method*, and *maximum-likelihood method*.

2.5.1 Coherent Signal Subspace Method (CSM)

Coherent signal subspace method for the wide-band source localization is proposed in [13]. This method can be applied for both coherent and incoherent source signals unlike the incoherent signal subspace method (ISM) in [12]. The main idea of the CSM is to gather the data collected from individual sensors at a central node, where we can compute the DFT of the collected data, divide spectral information into subbands, construct the correlation matrix for the spectral vectors, compute the associated singular-

value decomposition (SVD), and estimate the propagation delays accordingly. We may apply the focusing matrices (the collections of the principal singular vectors) to transform the original wide-band subspaces into the narrow-band signal subspaces and employ the MUSIC algorithm for the transformed narrow-band signals [15].

Consider an array of P sensors that collects the signals from M wide-band sources. The acquired signal vector at all sensors has a spatial spectral density matrix $\overline{P}_{xx}(k) = \overline{A}(f)\overline{P}_s(k)\overline{A}^H(k)$, where $\overline{A}(f) = \left[\underline{a}^{(1)}, \cdots, \underline{a}^{(M)}\right]$ is a $P \times M$ source-to-array matrix and its m^{th} column is $\underline{a}^{(m)} \equiv \underline{a}(x^{(m)}, y^{(m)}, k)$ relating the k^{th} frequency component of the m^{th} source to the P sensor signals.

Define

$$\begin{aligned}\underline{a}^{(m)} &\equiv \underline{a}(x^{(m)}, y^{(m)}, k)^H \\ &= \left[e^{-j2\pi k t_1^{(m)}}, e^{-j2\pi k t_2^{(m)}}, \cdots, e^{-j2\pi k t_p^{(m)}} \right],\end{aligned}$$

where $t_p^{(m)} \equiv \sqrt{(x^{(m)} - x_p)^2 + (y^{(m)} - y_p)^2} \Big/ v$ and (x_p, y_p) is the location of sensor p, $p = 1, \cdots, P$. $\left(x^{(m)}, y^{(m)}\right)$ is the location of source m, $m = 1, \cdots, M$. v is the propagation speed in the air. $\overline{P}_s(k)$ is the cross-spectral density matrix of the sources [13]. The steps to determine $\overline{P}_{xx}(k)$ is given as follows:

- Divide each sensor signal $x_p(n)$ into L sub-sequences $x_{pl}(n) \equiv x(nL + l)$, $p = 1, \cdots, P$, $l = 1, \cdots, L$, $n \in \mathsf{Z}$.
- Compute the discrete Fourier transform $X_{pl}(k)$, $k = 1, \cdots, K$, for $x_{pl}(n)$, where K is the DFT window size.

- Calculate the energy $\sum_{l=1}^{L}\sum_{p=1}^{P} X_{pl}(k)^2$ over K frequency bins, and select the J frequency bins j with highest energy, $j = 1, \cdots, J$, from the K frequency bins. J is a user-defined parameter.

- Estimate the spatial spectral density matrix $\hat{\bar{P}}_{xx}(j) = \frac{1}{L}\sum_{l=1}^{L} \underline{X}_l(j)\underline{X}_l^H(j)$ at frequency j, $j = 1, \cdots, J$, where $\underline{X}_l(j) \equiv [X_{1l}(j), \cdots, X_{Pl}(j)]^T$.

After determining the spatial spectral density matrix, we make use of the signal subspace property to determine the accurate steering vectors that are orthogonal to the null subspace and then estimate the source locations. First, the SVD of $\hat{\bar{P}}_{xx}(j)$ at the previously selected frequencies j, $j = 1, \cdots, J$, can be carried out as

$$\hat{\bar{P}}_{xx}(j) = \left[\bar{U}_s(j)\, \bar{U}_n(j)\right] \begin{bmatrix} \bar{\Sigma}_s & 0 \\ 0 & \bar{\Sigma}_n \end{bmatrix} \begin{bmatrix} \bar{U}_s^H(j) \\ \bar{U}_n^H(j) \end{bmatrix}, \tag{2.4}$$

where the singular vector matrices $\bar{U}_s(j)$ and $\bar{U}_n(j)$ correspond to the signal and noise subspaces, respectively, for frequency j. Then, for each location point (x, y), we evaluate

$$P^{(1)}(x, y) = \sum_{j=1}^{J} \frac{1}{\left| b(x, y, j)^H U_n(j) \right|}, \tag{2.5}$$

where $b(x, y, j) \equiv \left[e^{-j2\pi j t_1}, \cdots, e^{-j2\pi j t_P}\right]^M$, $t_p \equiv \sqrt{(x - x_p)^2 + (y - y_p)^2}\,/v$, and (x_p, y_p) is the location of sensor p, $p = 1, \cdots, P$. The indicator function $P^{(1)}(x, y)$ will yield a high peak as it steers to the correct source location and the source signal's correct frequency.

This CSM can also be used for the coherent source localization unlike the ISM. However, the preprocessor is needed in this method and brings additional computational burden.

2.5.2 Time-Delay Estimation Method

Time delay estimation makes use of time delay of arrival (TDOA) to estimate the target locations. TDOA is often employed for near field and wideband source localization and has been extensively investigated in [16-19].

The TDOA-based localization takes advantage of the propagation of the sound wave. Sound travels generally at a speed of 345m/s in air. The signal generated by the acoustic source reaches the sensors at various locations with different amount of time delays. These relative time delays between sensor data are estimated in the first step. In the second step, source localization is found using the estimated time delays.

Consider a sensor array of *P+1* sensors placed at $r_p \equiv (x_p, y_p, z_p)^T, p = 0, \cdots, N,$ in the three-dimensional space. The reference sensor is assumed to be located at the origin, i.e. $\underline{r_0} = (x_0, y_0, z_0)^T$. The acoustic source is assumed to be located at $\underline{r}^{(s)} \equiv (x^{(s)}, y^{(s)}, z^{(s)})^T$. The ranges from the origin to the p^{th} sensor and the sources are denoted by R_i and $R^{(s)}$, respectively.

$$R_i \equiv \left\| \underline{r_p} \right\|, \quad p = 0, \quad \cdots, \quad N, \tag{2.6}$$

$$R^{(s)} \equiv \left\| \underline{r}^{(s)} \right\|. \tag{2.7}$$

The distance between the source and the p^{th} sensor is denoted by,

$$D_p \equiv \left\| \underline{r_p} - \underline{r}^{(s)} \right\|. \tag{2.8}$$

We have the basic relation among the range difference between sensors *i* and *j* from the source :

$$d_{ij} \equiv D_i - D_j, \quad i, j = 0, \cdots, P. \tag{2.9}$$

The d_{ij} is proportional to the time-delay of arrival t_{ij} with the speed of propagation of sound *v*, $d_{ij} = v t_{ij}$.

The localization problem here then is to detrmine $\underline{r}^{(s)}$ given the set of $\left\{ \underline{r}_p \right\}$ and t_{ij}. The range difference d_{io} defines a hyperboloid by,

$$D_i - D_0 = \left\| \underline{r_i} - \underline{r}^{(s)} \right\| - \left\| \underline{r_0} - \underline{r}^{(s)} \right\| = d_{i0}, \quad i = 1, \cdots, P. \tag{2.10}$$

Given the set of range difference estimates $\underline{d} = (d_{10}, d_{20}, \cdots, d_{P0})^T$, we can determine the location of the acoustic wideband source by intersecting these hyperboloids but it is higly non-linear to solve. The one step least square (OSLS) algorithm is proposed by the authors for the aforementioned non-linearity problem in the paper [30].

From the Pythagorean theorem and Eq. (2.9) in Eq. (2.8),

$$\underline{r}_p^T \underline{r}^{(s)} + d_{po} R^{(s)} = \frac{1}{2}\left(R_p^2 - d_{p0}^2 \right), \qquad p = 1, \cdots, P. \tag{2.11}$$

According to Eq. (2.11), the *P* equations can be written in matrix form as

$$\overline{A}\Theta = \underline{b}, \tag{2.12}$$

where,

$$\overline{A} \equiv \left[\overline{S} \mid \underline{d} \right], \quad \overline{S} \equiv \begin{bmatrix} x_1 & y_1 & z_1 \\ x_2 & y_2 & z_2 \\ \vdots & & \\ x_P & y_P & x_P \end{bmatrix}, \; \Theta \equiv \begin{bmatrix} x^{(s)} \\ y^{(s)} \\ z^{(s)} \\ R^{(s)} \end{bmatrix}, \; \underline{b} \equiv \frac{1}{2} \begin{bmatrix} R_1^2 - d_{10}^2 \\ R_2^2 - d_{20}^2 \\ \vdots \\ R_P^2 - d_{P0}^2 \end{bmatrix}.$$

The above spherical equations are linear in $\underline{r}^{(s)}$ given $R^{(s)}$ and vice versa. The OSLS is regarded as least-square method, which computes the source location in single step. Thereby, OSLS decreases the computational complexity without sacrificing the statistical estimation accuracy. The OSLS solution for Θ is given by :

$$\hat{\Theta} = (\overline{A}^T \overline{A})^{-1} \overline{A}^T \underline{b}. \tag{2.13}$$

Eq. (2.15) can be also written as,

$$\hat{\Theta} = \left[\begin{array}{c|c} \overline{S}^T \overline{S} & \overline{S}^T \underline{d} \\ \hline \underline{d}^T \overline{S} & \underline{d}^T \underline{d} \end{array} \right]^{-1} \left[\begin{array}{c} \overline{S}^T \\ \hline \underline{d}^T \end{array} \right] \underline{b}. \tag{2.14}$$

Projection matrix onto *d*-orthogonal is given as

$$P_{d\perp} \equiv I - \frac{\underline{d}\,\underline{d}^T}{\underline{d}^T \underline{d}}, \tag{2.15}$$

and estimate the source location $\hat{\underline{r}}^{(s)}$ as

$$\hat{r}^{(s)} = (\overline{S}^T P_{d\perp} \overline{S})^{-1} \overline{S}^T P_{d\perp} \underline{b}, \tag{2.16}$$

which minimizes the following difference function

$$J(r^{(s)}) = \left\| P_{d\perp} \underline{b} - P_{d\perp} \overline{S} r^{(s)} \right\|. \tag{2.17}$$

The method given by Eqs. (2.14-2.17) is a good alternative for the CSM method discussed earlier. This method is less reliable if the source localization problem deals with multiple sources as it is very difficult to calculate the relative time delays of each individual source at each sensor node.

2.5.3 Maximum-Likelihood Estimation Method

Maximum-likelihood estimation for the source location parameters has been acknowledged as the optimal and robust technique. In this method, the likelihood function of the sensor signals is evaluated at the each location point in the uniform searching grid, and then the source location is determined according to the spot with the maximum likelihood.

According to [6], we consider a randomly distributed array of P sensors to collect the data from M sources. Since the sources are assumed to be in the near field, the signal gains are different across the sensors. Then, the signal collected by the p^{th} sensor at time n is given by

$$x_p(n) = \sum_{m=1}^{M} a_p^{(m)} s_0^{(m)}\left(n - t_p^{(m)}\right) + w_p(n), \tag{2.21}$$

for $n = 0,1,\cdots,L-1$, $p = 1,\cdots,P$, $m = 1,\cdots,M$, where

$a_p^{(m)}$ is the signal gain of the m^{th} source at the p^{th} sensor;

$s_0^{(m)}$ denotes the m^{th} source signal waveform;

$t_p^{(m)}$ is the propagation delay in samples from the p^{th} sensor to the m^{th} source;

$w_p(n)$ represents the zero-mean independently identically distributed Gaussian noise process with variance σ^2. Several location parameters can be specified as follows:

$t_p^{(m)} = \dfrac{\left\| \underline{r_s}^{(m)} - \underline{r_p} \right\|}{v}$ (propagation delay),

$\underline{r_s}^{(m)} \in \mathsf{R}^{2\times 1}$: the m^{th} source location,

$\underline{r_p}$: the p^{th} sensor location,

v: the speed of propagation in meters/sec. Taking the DFT for both sides of Eq. (2.21), we have

$$\underline{X}(k) = \overline{D}(k)\underline{S_0}(k) + \underline{U}(k),\ k = 0,1,\cdots,N-1, \tag{2.22}$$

where

$\underline{X}(k) \equiv \left[X_1(k) \quad \cdots \quad X_P(k)\right]^T \in \mathbb{C}^{P\times 1}$ ($X_p(k)$ is the k^{th} DFT point of $x_p(n)$, $p = 1,\cdots,P$);

$\overline{D}(k) \equiv \left[\underline{d}^{(1)}(k) \quad \cdots \quad \underline{d}^{(M)}(k)\right] \in \mathbb{C}^{P\times M}$ consists of M steering vectors, each given by

$$\underline{d}^{(m)}(k) \equiv \left[d_1^{(m)}(k) \quad \cdots \quad d_P^{(m)}(k)\right]^T \in \mathbb{C}^{P\times 1}$$

and

$$d_p^{(m)} \equiv a_p^{(m)} e^{-j2\pi t_p^{(m)}/N};$$

$\underline{S_0}(k) \equiv \left[S_0^{(1)}(k) \quad \cdots \quad S_0^{(M)}(k)\right]^T \in \mathbb{C}^{M\times 1}$ ($S_0^{(m)}(k)$ is the k^{th} DFT point of $s_0^{(m)}$, $m = 1,\cdots,M$).

The source signal spectra $\underline{S_0}(k)$ are unknown and deterministic. The noise spectral vector $\underline{U}(k) \in \mathbb{C}^{P\times 1}$ is a complex-valued zero-mean white Gaussian process and each element has a variance $L\sigma^2$.

Here, the unknown parameter vector $\underline{\Theta} \in \mathbb{C}^{(MN+2M)\times 1}$ is

$$\underline{\Theta} = \left[\underline{r_s}^T, \underline{S_0}^{(1)^T} \quad \cdots \quad \underline{S_0}^{(m)^T} \quad \cdots \quad \underline{S_0}^{(M)^T}\right]^T,$$

where

$$\underline{r_s} \equiv \left[\underline{r_s}^{(1)T} \quad \cdots \quad \underline{r_s}^{(m)T} \quad \cdots \quad \underline{r_s}^{(M)T} \right]^T \in \mathsf{R}^{1\times 2M}$$

and

$$\underline{S_0}^{(m)} \equiv \left[S_0^{(m)}(0) \quad \cdots \quad S_0^{(m)}(N-1) \right]^T \in \mathsf{C}^{N\times 1}.$$

According to Eq. (2.22), we may construct the equivalent log-likelihood of $\underline{X}(k)$ after neglecting the constant terms, which is given by

$$\begin{aligned} J(\underline{r_s}) &= \log f_{\underline{X}}\left[\underline{\Theta};\, \underline{X}(k)\right] \\ &\equiv -\sum_{k=1}^{N} \left[\underline{X}(k) - \overline{D}(k)\underline{S_0}(k)\right]^H \left[\underline{X}(k) - \overline{D}(k)\underline{S_0}(k)\right]. \end{aligned} \tag{2.23}$$

Thus, the maximum-likelihood estimation of $\underline{\Theta}$ can be achieved as

$$\begin{aligned} \underline{\hat{\Theta}} &= \arg\max\left(\log f_{\underline{X}}\left[\underline{\Theta};\, \underline{X}(k)\right]\right) \\ &= \arg\min\left(\sum_{k=0}^{N-1} \left[\underline{X}(k) - \overline{D}(k)\underline{S_0}(k)\right]^H \left[\underline{X}(k) - \overline{D}(k)\underline{S_0}(k)\right]\right). \end{aligned} \tag{2.24}$$

Eq. (2.24) yields the source signal spectral estimates as

$$\underline{\hat{S}_0}(k) = (\overline{D}(k)^H \overline{D}(k))^{-1} \overline{D}(k)^H \underline{X}(k). \tag{2.25}$$

According to [6] and Eqs. (2.23), (2.25), the ML source location estimates can be obtained as

$$\arg\max\left(J(\underline{r_s})\right) = \arg\min\left(\sum_{k=0}^{N-1} \left\| \overline{P}(k, \underline{r_s})\underline{X}(k) \right\|^2\right), \tag{2.26}$$

where the *projection matrix* $\overline{P}(k, \underline{r_s})$ is defined as

$$\overline{P}(k, \underline{r_s}) \equiv \overline{D}(k)(\overline{D}(k)^H \overline{D}(k))^{-1} \overline{D}(k)^H.$$

For the single source case, the ML estimator in Eq. (2.26) can be further simplified as

$$\arg\max\left(J(\underline{r_s})\right) \equiv \arg\min\left(\sum_{k=0}^{N-1}\left|B(k,r_s)\right|^2\right), \tag{2.27}$$

where $B(k,r_s) = \underline{d}(k,r_s)^H \underline{X}(k)$ is a scalar. It is obvious that the cost function $J(\underline{r_s})$ in Eq. (2.26) is nonlinear for multiple sources. Hence, we propose to adopt the EM procedure to solve Eq. (2.26).

Chapter 3 Signal Analysis in the Frequency Domain

The frequency analysis arises as a matter of fact that the wide-band signal is distributed over a broad range of frequencies and the signal is difficult to be characterized thereby. Therefore, in this thesis, we utilize the discrete-Fourier transform (DFT) filter bank to decompose the wide-band signals collected by the sensors and then apply the attained spectral information to estimate the complete set of parameters such as source waveforms and source locations. In this chapter, we introduce the usual frequency analysis tool, the Fourier transform.

3.1 Discrete Fourier Transform

The frequency analysis of the discrete-time signals generally relies on a digital signal processor, which may be personal computer or specially-designed logic circuits. The frequency analysis of a discrete-time signal $x(n)$ is undertaken by converting the time series into its spectral representation $X(\omega)$. Then we sample $X(\omega)$, which is a continuous function, to generate another discrete sequence $X(k)$. Consider a discrete-time signal $x(n)$, $n = -\infty, \quad \cdots, \quad \infty$. Then the discrete-time Fourier transform of $x(n)$ is given by

$$X(\omega) = \sum_{n=-\infty}^{\infty} x(n) e^{-j\omega n} . \qquad (3.1)$$

Assume that $X(\omega)$ is sampled with frequency gap $\delta\omega$ radians between the consecutive samples. Now, $X(\omega)$ is periodical with period 2π. If we consider *N* equidistant samples in the interval $0 \le \omega < 2\pi$ with such a spacing $\delta\omega = 2\pi / N$,

Then the sampled frequency response is

$$X\left(\frac{2\pi}{N} k\right) = \sum_{n=-\infty}^{\infty} x(n) e^{-j2\pi kn/N}, \quad k = 0,1, \quad \cdots, \quad N-1. \qquad (3.2)$$

The above equation is easily divided into infinite number of summations as given below

$$X\left(\frac{2\pi}{N}k\right) = \cdots + \sum_{n=-N}^{-1} x(n)e^{-j2\pi kn/N} + \sum_{n=0}^{N-1} x(n)e^{-j2\pi kn/N} + \sum_{n=N}^{2N-1} x(n)e^{-j2\pi kn/N} + \cdots$$
$$= \sum_{l=-\infty}^{\infty} \sum_{n=lN}^{lN+N-1} x(n)e^{-j2\pi kn/N}. \tag{3.3}$$

Eq. (3.3) can yield

$$X\left(\frac{2\pi}{N}k\right) = \sum_{n=0}^{N-1}\left[\sum_{l=-\infty}^{\infty} x(n-lN)\right] e^{-j2\pi kn/N}, \text{ for } k = 0,1,2, \cdots, N-1. \tag{3.4}$$

Let $x_p(n) \equiv \sum_{l=-\infty}^{\infty} x(n-lN)$, where $x_p(n)$ is obtained by the periodic extension of $x(n)$ the with period N.

The DFT samples in Eq. (3.4) correspond to a periodic sequence $x_p(n)$, where a single period of $x_p(n)$ is given by

$$x_p(n) = \begin{cases} x(n), & 0 \le n \le L-1 \\ 0, & L \le n \le N-1 \end{cases}. \tag{3.5}$$

Eq. (3.5) means that the DFT $X\left(\frac{2\pi}{N}k\right)$, $k = 0,1,2, \cdots, N-1$, can only characterize the finite-duration sequence $x(n)$ of length *N*. Similarly, for a finite-duration signal $x(n)$ of length *N*, the corresponding DFT is

$$X(k) = X\left(\frac{2\pi}{N}k\right) = \sum_{n=0}^{N-1} x(n)e^{-j2\pi kn/N}, \quad k = 0, 1, \cdots, N-1. \tag{3.6}$$

Eq. (3.6) is used to decompose the sensor signals into different narrow-band frequency bins.

Chapter 4 Expectation Maximization for Source Localization

4.1 EM Algorithm

Expectation maximization (EM) algorithm is an alternative to search for the maximum-likelihood parameter estimates when the ML problem is complex and non-linear. We would like to discuss the generic EM algorithm in [31] as a start of this chapter.

4.1.1 Maximum-likelihood Problem

Consider a density function $p(x|\Theta)$ which is dependant of the set of parameters Θ (e.g., x might be a Gaussian mixture process and Θ could be the means and co-variances). A data set of size N is drawn from the underlying statistics, i.e., $X = \{x_1, \cdots, x_N\}$. In addition, we assume that these data constitute an independently and identically distributed (i. i. d.) process with the probability density function $p(x|\Theta)$. Therefore, the probability density function for the data samples is

$$p(X|\Theta) = \prod_{i=1}^{N} p(x_i|\Theta) = L(\Theta|X). \tag{4.1}$$

This function $L(\Theta|X)$ is also regarded as the likelihood of the parameters given the data, or just the *likelihood function*. This likelihood can be seen as a function of the parameter set Θ while the data X is known. The aim of the maximum likelihood problem is to find the optimal Θ that maximizes $L(\Theta|X)$, such that

$$\Theta^* = \arg\max_{\Theta}\left[L(\Theta|X)\right]. \tag{4.2}$$

Often we maximize the log-likelihood $\log[L(\Theta|X)]$ instead due to its simplicity. The formula of $p(x|\Theta)$ determine the complexity of the ML problem. For example, if $p(x|\Theta)$ is simply a Gaussian distribution where $\Theta = (a,b)$, then we can set the derivative of $\log[L(\Theta|X)]$ to zero, and analytically solve a^* and b^*. However, usually it is not possible to reach such analytical expressions for many other distribution functions, and we must rely on the sophisticated elaboration for the ML search.

4.1.2 General EM Algorithm

The EM algorithm is a general method for determining the maximum-likelihood estimates of the parameters from a given data set and a given underlying distribution function when the data is incomplete or possess latent variables. The EM algorithm is applied for the two common situations: (*i*) some data samples are missing in the observation process; (*ii*) the ML estimation is not analytically achievable but it can be simplified by assuming the existence of some hidden variables or parameters. Similarly, we assume that data *X* is observed and it is generated by an underlying distribution. We call *X* the *incomplete data*. Then, we assume that a complete data set exists such that *Z* = (*X, Y*) and a joint density function is specified as

$$p(z \mid \Theta) = p(x, y \mid \Theta) p(x \mid \Theta). \tag{4.3}$$

This joint density function $p(z \mid \Theta)$ depends on the marginal density function $p(x \mid \Theta)$ and the assumption of latent variables. In other cases involving missing data samples in observation, we must assume a relationship between *x* and *y*. With this new density function $p(z \mid \Theta)$, we can define a new likelihood function, $L(\Theta \mid Z) = L(\Theta \mid X, Y) = p(X, Y \mid \Theta)$, which is called the complete-data likelihood. Here,

it should be noted that this function $L(\Theta \mid Z)$ is random since the missing data (or latent variable) Y is unknown, random, and governed by an underlying distribution. For differentiation, the original likelihood $L(\Theta|X)$ is referred to as the incomplete-data likelihood function.

For the $(i\text{-}1)^{th}$ iteration, the EM algorithm first determines the expected value of the complete-data log-likelihood $p(X,Y \mid \Theta)$ with respect to the unknown data Y given the observed data X and the current parameter estimates $\Theta^{(i-1)}$. It is also called the E-step. That is, we define

$$Q(\Theta,\Theta^{(i-1)}) \equiv E\left[\log p(X,Y \mid \Theta) \mid X,\Theta^{(i-1)}\right], \qquad (4..4)$$

where $\Theta^{(i-1)}$ correspond to the current parameters estimates that we use to evaluate the expectation in Eq. (4.4) and Θ correspond to the new parameters to increase $Q(\Theta,\Theta^{(i-1)})$ during the ML procedure. Eq. (4.4) needs further clarifications. It is noted that both X and $\Theta^{(i-1)}$ are known, Θ is a adjustable variable while Y is a random variable governed by the distribution $f(y \mid X,\Theta^{(i-1)})$. The right side of Eq. (4.4) can therefore be rewritten as

$$E\left[\log p(X,Y \mid \Theta) \mid X,\Theta^{(i-1)}\right] = \int_{y\in Y} \log p(X,y \mid \Theta) f(y \mid X,\Theta^{(i-1)}) dy. \qquad (4.5)$$

Note that $f(y \mid X,\Theta^{(i-1)})$ is the marginal distribution of the incomplete data and is dependent on both observed data X and on current parameters $\Theta^{(i-1)}$, and Y is the domain of values y can take on. This marginal distribution $f(y \mid X,\Theta^{(i-1)})$ is a simple analytical expression of the current parameters $\Theta^{(i-1`)}$ and the observed data X.

The calculation of the expectation $E\left[\log p(X,Y|\Theta)|X,\Theta^{(i-1)}\right]$ is called the E-step of the EM algorithm. We need to clearly differentiate the two arguments in the function $Q(\Theta,\Theta^{(i-1)})$. The first argument Θ corresponds to the parameters which will finally be optimized for the iterative likelihood maximization. The second argument $\Theta^{(i-1)}$ corresponds to the parameters which will be used to evaluate the expectation.

The second step (M-step) of the EM algorithm is to maximize the expectation we calculate from the first step. That is, we determine

$$\Theta^{(i-1)} = \arg\max_{\Theta} Q(\Theta,\Theta^{(i-1)}). \tag{4.6}$$

Thus, these two steps (E- and M-steps) are repeated on after another for a fixed number of iterations. In each iteration, the log-likelihood measure is guaranteed to increase from the previous iteration and the EM algorithm will converge to a local maximum of the likelihood function.

A new modeled M-step procedure can be undertaken that we can apply any algorithm to search $\Theta^{(i)}$ such that $Q(\Theta^{(i)},\Theta^{(i-1)}) > Q(\Theta,\Theta^{(i-1)})$ rather than directly maximize $Q(\Theta,\Theta^{(i-1)})$. The generalized EM algorithm can be formed with this modified M-step and it is also guaranteed to converge. However, the variations of EM algorithm for different problems cannot be exhaustively discussed in this thesis and they have quite different formulations in general.

4.2 EM Algorithm for Wideband Signal Source Localization

The EM algorithm is a well-known iterative algorithm for the maximum-likelihood estimation. The complicated nonlinear optimization problem in Eq. (2.26) can be simplified using the EM procedure incorporated with the augmented (complete) data

corresponding to individual incident source signals. First, we denote the received signal spectrum (the k^{th} DFT point of $a_p^{(m)} s_0^{(m)}\left(n - t_p^{(m)}\right)$) as $X_p^{(m)}(k)$, $1 \le p \le P, 1 \le m \le M, 0 \le k \le N-1$, from the m^{th} source to the p^{th} sensor. Then we define the augmented data as $\{\underline{X}^{(m)}(k); 1 \le m \le M, 0 \le k \le N-1\}$,

where

$$\underline{X}^{(m)}(k) = [X_1^{(m)}(k), ..., X_P^{(m)}(k)]^T \in \mathbb{C}^{P \times 1}.$$

In addition, we assume that is a mixture Gaussian process with the cluster mean vectors $\underline{d}^{(m)}(k) S_0{}^{(m)}(k)$ identical cluster covariance matrices $(1/M)\sigma^2 \bar{I}$ where $\bar{I}$ denotes the $P \times P$ identity matrix. The relationship between the observed (incomplete) data $\underline{X}(k)$ and the complete data is established as

$$\underline{X}(k) = \sum_{m=1}^{M} \underline{X}^{(m)}(k). \tag{4.7}$$

Then the log-likelihood function of the defined complete data can be written as

$$\begin{aligned} &\log f_{\underline{X}}\left[\Theta; \underline{X}^{(m)}(k)\right] \\ &\quad \equiv -\sum_{k=0}^{N-1} \sum_{m=1}^{M} \left| \underline{X}^{(m)}(k) - \underline{d}^{(m)}(k) S_0{}^{(m)}(k) \right|^2. \end{aligned} \tag{4.8}$$

We re-write Eq. (4.8) as

$$\log f_{\underline{X}}\left[\Theta; \underline{X}^{(m)}(k)\right] = -\sum_{m=1}^{M} f_{\underline{x}^{(m)}}(\underline{r_s}^{(m)}, \underline{S_0}^{(m)}), \tag{4.9}$$

where

$$f_{\underline{x}^{(m)}}(\underline{r_s}^{(m)}, \underline{S_0}^{(m)}) \equiv \sum_{k=0}^{N-1} \left| \underline{X}^{(m)}(k) - \underline{d}^{(m)}(k) S_0{}^{(m)}(k) \right|^2,$$

and $S_0^{(m)}(k)$ depends on $\underline{S_0}^{(m)}$ and $\underline{d}^{(m)}(k)$ depends on $\underline{r_s}^{(m)}$ as discussed in Section II.

The log-likelihood of complete data given by Eq. (4.9) is a summation of the individual log-likelihood functions of the multiple incident sources. Since the individual log-likelihood $\log f_{\underline{x}^{(m)}}(\underline{r_s}^{(m)}, \underline{S_0}^{(m)})$ depends only on $\underline{r_s}^{(m)}$, the maximization of $\log f_{\underline{X}}\left[\Theta; \underline{X}^{(m)}(k)\right]$ can be performed by maximizing each individual $\log f_{\underline{x}^{(m)}}(\underline{r_s}^{(m)}, \underline{S_0}^{(m)})$ separately. As a result, the unknown parameter to be estimated in $\log f_{\underline{x}^{(m)}}(\underline{r_s}^{(m)}, \underline{S_0}^{(m)})$ is solely $\underline{r_s}^{(m)}$. It means that there is no need of multivariate search of $\underline{r_s}^{(m)}$, $m = 1, \cdots, M$ altogether in the 2*M*-dimensional space simultaneously for all source locations.

Since complete data $\underline{X}^{(m)}(k)$ are not available, the expectation has to be performed using the current estimated parameters. Given the estimate $\Theta^{[i]}$ for the i^{th} iteration, the $(i+1)^{\text{th}}$ iteration of EM algorithm involves the following two steps:

Expectation (E-step)

Calculate

$$Q(\Theta, \Theta^{[i]}) = E\left\{\log f_{\underline{X}}\left[\Theta; \hat{\underline{X}}^{(m)}(k, \Theta^{[i]})\right]\right\}, \text{ for } m = 1, \cdots, M, \tag{4.10}$$

where

$$\begin{aligned} \hat{\underline{X}}^{(m)}(k, \Theta^{[i]}) &\equiv E\left[\underline{X}^{(m)}(k) \mid \underline{X}, \Theta^{[i]}\right] \\ &= \underline{d}^{(m)}(k) S_0^{(m)}(k) + \frac{1}{M}(\underline{X}(k) - \overline{D}(k)\underline{S_0}(k)). \end{aligned} \tag{4.11}$$

It is noted that $\underline{d}^{(m)}(k)$, $S_0^{(m)}(k)$, $\overline{D}(k)$, $\underline{S_0}(k)$, $k = 0,1,\cdots,N-1$, are all estimated using $\hat{\underline{r}}_s^{(m)}$ obtained from the previous iteration *i*, according to the definitions below Eq. (2.2).

Maximization (M-step):

Re-estimate

$$\hat{\underline{r}}_s^{(m)} = \arg\max_{\underline{r}_s^{(m)}} \sum_{k=0}^{N-1} \left| \left[\underline{d}^{(m)}(k)\right]^H \hat{\underline{X}}^{(m)}(k, \Theta^{[i]}) \right|^2, \tag{4.12}$$

$$\hat{S}_0^{(m)}(k) = \frac{\left[\underline{d}^{(m)}(k)\right]^H \hat{\underline{X}}^{(m)}(k, \Theta^{[i]})}{\left\|\underline{d}^{(m)}(k)\right\|^2}, \tag{4.13}$$

for $m = 1,\cdots,M$, $k = 0,1,\cdots,N-1$.

Then update

$$\Theta^{[i+1]} = \left[\hat{\underline{r}}_s^{\,T}, \hat{\underline{S}}_0^{(1)T} \quad \cdots \quad \hat{\underline{S}}_0^{(m)T} \quad \cdots \quad \hat{\underline{S}}_0^{(M)T} \right]^T,$$

where

$$\hat{\underline{r}}_s \equiv \left[\hat{\underline{r}}_s^{(1)T} \quad \cdots \quad \hat{\underline{r}}_s^{(m)T} \quad \cdots \quad \hat{\underline{r}}_s^{(M)T} \right]^T,$$

and

$$\hat{\underline{S}}_0^{(m)} \equiv \left[\hat{S}_0^{(m)}(0) \quad \cdots \quad \hat{S}_0^{(m)}(N-1) \right]^T,$$

for $m = 1,\cdots,M$. The E- and M-steps are repeated until the pre-defined convergence of the estimated parameters are achieved.

Eqs. (4.11)-(4.13) yield a recursive solution for multiple wide-band source localization. The source locations are randomly initiated. We carry out the expectation

according Eq. (4.11) and then undertake the maximization of the log-likelihood function using Eq. (4.13) to update the estimates of the source locations $\underline{\hat{r}}_s^{(m)}$. We continue the aforementioned EM iterations until the convergence is reached. Observe Eqs. (4.11), (4.12) that we can maximize the log-likelihood functions in parallel to estimate the source locations $\underline{\hat{r}}_s^{(m)}$, $m = 1, \cdots, M$, simultaneously. Thus, the computational time can be greatly reduced using the distributed computations.

Chapter 5 Simulations and Results

We present the comparison between our new proposed EM-based multiple wide-band source localization scheme with the alternating projection method here. Acoustic source signal is acquired from [6]. The sampling frequency is 100 kHz. The propagation speed is 345 meters/sec. The data is simulated for a circularly-shaped array of five sensors using the recoded acoustic data from [6] as shown in Figure 1 (squares denote the sensor locations, circles denote the actual source locations). Two equal energy sources are assumed for the simulation.The sample size is L = 200, and the DFT size is N = 256. Two-dimensional grid point search is employed, where both x- and y-axes are uniformly sampled.

Fifty Monte Carlo experiments are carried out using randomly initiated source location estimates for a particular signal-to-noise ratio (SNR=20 dB). The localization result from an arbitrary trial is also depicted in Figure 5.1. Figures 5.2 and 5.3 depict the individual likelihoods $\log f_{\underline{x}^{(m)}}(\underline{r_s}^{(m)}, \underline{S_0}^{(m)})$, m=1, 2, respectively. It is obvious that the unique peaks (source locations) can be easily found in both figures.

The root-mean-square (RMS) estimation errors for individual sources using our EM algorithm and the conventional AP method, for different signal-to-noise ratios ranging from 5 to 30 dB, are calculated among the 50 Monte Carlo experiments and depicted in Figure 5.4. According to Figure 5.4, our EM algorithm achieves more precise results than the AP method. However, these results are subject to the appropriate initialization.

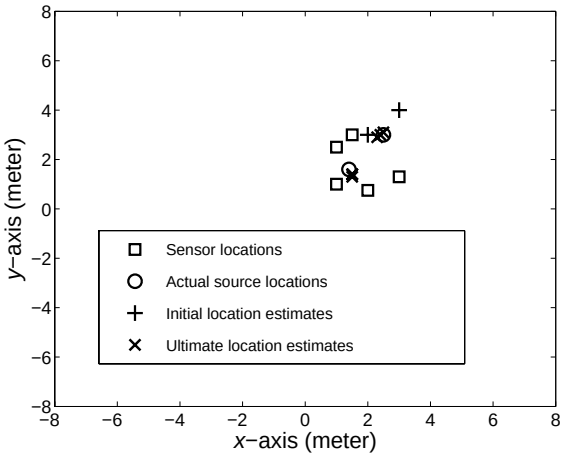

Figure 5.1 Localization of two wide-band sources in the near field (signal-to-noise ratio is 20 dB, grid resolution is 0.1×0.1 squared meters).

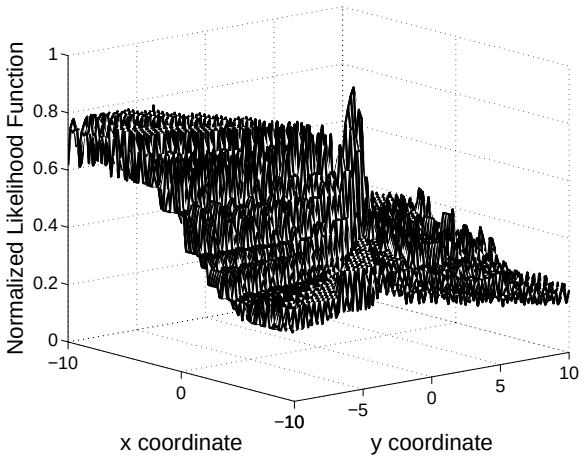

Figure 5.2 Three-dimensional plot for the first individual log-likelihood (signal-to-noise ratio is 20 dB, grid resolution is 0.1×0.1 squared meters).

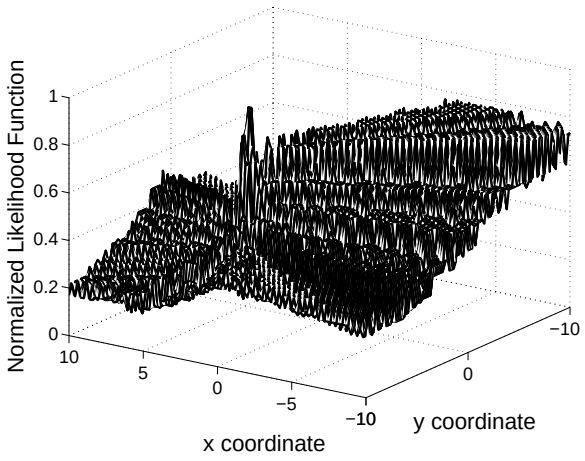

Figure 5.3 Three-dimensional plot for the second individual log-likelihood (signal-to-noise ratio is 20 dB, grid resolution is 0.1×0.1 squared meters).

Finally, we provide the computational complexity analysis in terms of complex multiplications here. Since the number iterations required for the EM and AP algorithm in for our initialization in the above results is same. So, we computed the number complex computations needed for the one iteration in the both the cases. The computational complexity for the AP method is $NM^2P^3N_xN_y$ where N_x, N_y denote the numbers of search points along *x*- and *y*-axes, respectively; whereas the computational complexity for our EM algorithm per iteration is $N\left(M^2P^3 + MP + N_xN_yMP^2\right)$. The computational complexity curves versus the number of sources M and the grid resolutions N_xN_y are depicted in Figures 5.5 and 5.6, respectively. Although we have not presented or tested the multiple source case involving more two sources, we assumed that the presented algorithm would work for the all other cases, which contain more than two sources, provided the proper number of sensors and

sensor array geometry. According to Figures 5.5, 5.6, the EM algorithm is much more efficient than the AP method. The difference can be up to one order-of-magnitude.

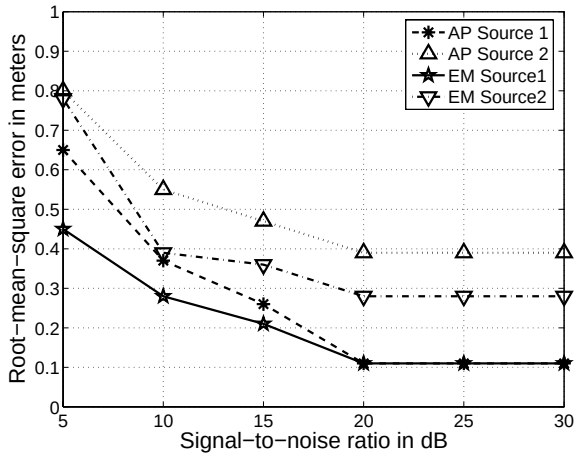

Figure 5.4 Comparison of the RMS-error v.s. SNR for the EM and AP schemes (grid resolution is 0.1×0.1 squared meters).

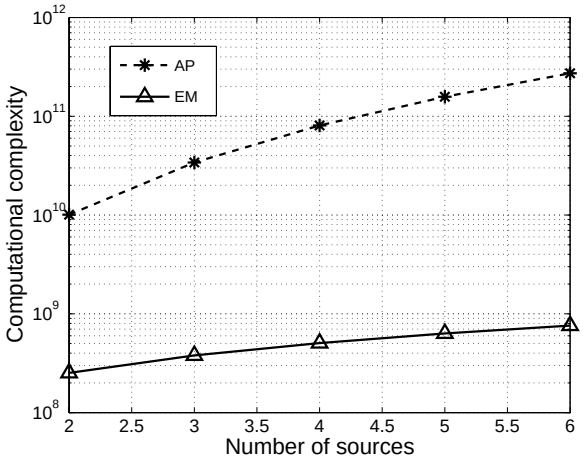

Figure 5.5Computational complexity comparison v.s. number of sources for the EM and AP schemes (signal-to-noise ratio is 20 dB, grid resolution is 0.1×0.1 squared meters).

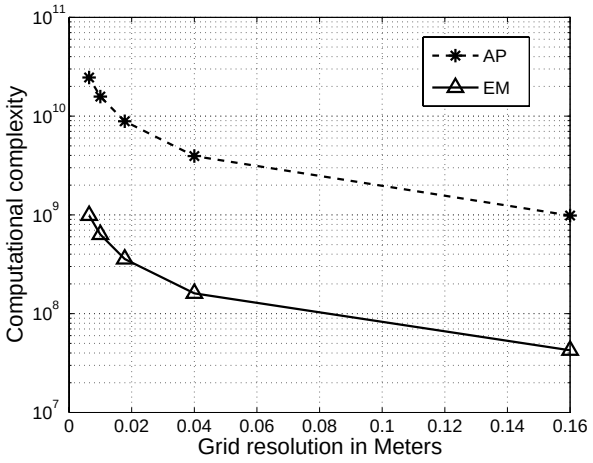

Figure 5.6 Computational complexity comparison v.s. grid resolution for the EM and AP schemes (two sources, signal-to-noise ratio is 20 dB).

Chapter 6 Conclusion

In this thesis, we propose a novel EM-based multiple wide-band source localization scheme. We performed simulation for the two source case surrounded by five sensors and showed that EM algorithm can outperform the conventional alternating projection method in terms of root-mean-square estimation error and computational complexity when proper initialization is provided. Besides, we can also decouple the multiple-source localization problem into the individual source localization sub-problems in parallel, which can greatly benefit from the modern distributive computation and yield a much less time-consuming solution. Our new promising technique can serve for the future energy-constrained sensor networks.

Bibliography

[1] J. Krim and M. Viberg, "Two decades of array signal processing research: the parametric approach," *IEEE Signal Processing Magazine*, vol.13, no. 4, pp. 67-94, July 1996.

[2] J. Capon, "High-resolution frequency-wavenumber spectrum analysis," *Proceedings of the IEEE*, vol. 57, no. 8, pp. 1408-1418, August 1969.

[3] R. O. Schmidt, "Multiple emitter location and signal parameter estimation," *IEEE Transactions on Antennas and Propagation*, vol. 34, no. 3, pp. 276-280, March 1986.

[4] S. S. Reddi, "Multiple source location - a digital approach," *IEEE Transactions on Aerospace Electronic Systems*, vol. 15, no. 1, pp. 95-105, January 1979.

[5] M. I. Miller and D. R. Fuhrmann, "Maximum-likelihood narrow-band direction finding and the EM algorithm," *IEEE Transactions on Acoustics, Speech, and Signal Processing*, vol. 38, no. 9, pp. 1560-1577, September 1990.

[6] J. C. Chen, R. E. Hudson and K. Yao, "Maximum-likelihood source localization and unknown sensor location estimation for wideband signals in the near-field," *IEEE Transaction on Signal Processing*, vol. 50, no. 8, pp. 1843-1854, August 2002.

[7] T. L. Tung, K. Yao, D. Chen, R. E. Hudson and C. W. Reed, "Source localization and spatial filtering using wideband MUSIC and maximum power beamforming for multimedia applications," in *Proceedings of IEEE Workshop on Signal Processing Systems*, pp. 625-634, October 1999.

[8] S. Valaee and P. Kabal, "Wideband array processing using a two-sided correlation transformation," *IEEE Transactions on Signal Processing*, vol. 43, no. 1, pp. 160-172, January 1995.

[9] S. Valaee, B. Champagne and P. Kabal, "Localization of wideband signals using least-squares and total least-squares approaches," *IEEE Transactions on Signal Processing*, vol. 47, no. 5, pp. 1213-1222, May 1999.

[10] H. Hung and M. Kaveh, "Focusing matrices for coherent signal-subspace processing," *IEEE Transaction on Acoustic, Speech, Signal Processing*, vol. 36, no. 8, pp. 1272-1281, August 1988.

[11] E. Cekli and H. A. Cirpan, "Unconditional maximum likelihood approach for localization of near-field sources: algorithm and performance analysis," *AEU International Journal of Electronics and Communications*, vol. 57, no. 1, pp. 9-15, January 2003.

[12] M. Wax, T. Shan, and T. Kailath, “Spatio-temporal spectral analysis by eigenstructure methods,” *IEEE Trans. Acoust., Speech, Signal Processing*, vol. ASSP-32, pp. 817–827, Aug. 1984.

[13] H. Wang, and M. Kaveh, “Coherent signal-subspace processing for the detection and estimation of angles of arrival of multiple wide-band sources,” *IEEE Trans. Acoust., Speech, Signal Processing*, vol. ASSP-33, pp. 823–831, Aug. 1985.

[14] H. Hung and M. Kaveh, “On the statistical sufficiency of the coherently averaged covariance matrix for the estimation of the parameters of wideband sources,” in *Proc. IEEE Int. Conf. Acoust., Speech, SignalProcess.*, 1987.

[15] R. O. Schmidt, “Multiple emitter location and signal parameter estimation,” *IEEE Trans. Antennas Propagat.*, vol. AP-34, pp. 276–280, Mar. 1986.

[16] H. C. Schau and A. Z. Robinson, “Passive source localization employing intersecting spherical surfaces from time-of-arrival differences,” *IEEE Trans. Acoust., Speech, Signal Processing*, vol. ASSP-35, pp. 1223–1225, Aug. 1987.

[17] J. O. Smith and J. S. Abel, “Closed-form least-squares source location estimation from range-difference measurements,” *IEEE Trans. Acoust.,Speech, Signal Processing*, vol. ASSP-35, pp. 1661–1669, Dec. 1987.

[18] Y. T. Chan and K. C. Ho, “A simple and efficient estimator for hyperbolic location,” *IEEE Trans. Signal Processing*, vol. 42, pp. 1905–1915, Aug.1994.

[19] M. S. Brandstein, J. E. Adcock, and H. F. Silverman, “A closed-form location estimator for use with room environment microphone arrays,” *IEEE Trans. Speech Audio Processing*, vol. 5, pp. 45–50, Jan. 1997.

[20] I. Ziskind and M. Wax, “Maximum likelihood localization of multiple sources by alternating projection,” *IEEE Transactions on Acoustics, Speech, and Signal Processing*, vol. 36, no. 10, pp. 1553-1560, October 1988.

[21] A. P. Dempster, N. M. Laird and D. B. Rubin, “Maximum likelihood from incomplete data via the EM algorithm,” *Journal of the Royal Statistical Society*, ser. B, vol. 39, no. 1, pp. 1-38, 1977.

[22] M. Feder and E. Weinstein, “Multipath and multiple source array processing via the EM algorithm,” *Proceedings of IEEE International Conference on Acoustics, Speech, and Signal Processing*, vol. 11, pp. 2503-2506, April 1986.

[23] M. Feder and E. Weinstein, “Parameter estimation of superimposed signals using the EM algorithm,” *IEEE Transactions on Acoustics, Speech, and Signal Processing*, vol. 36, no. 4, pp. 477-489 , April 1988.

[24] E. Weinstein, V. Oppenheim and M. Feder, "Iterative and sequential algorithms for multisensor signal enhancement," *IEEE Transactions on Signal Processing*, vol. 42, no. 4, pp. 846-859, April 1994.

[25] P. J. Chung and J. F. Bohme, "Recursive EM and SAGE algorithms," *Proceedings of IEEE Workshop on Statistical Signal Processing*, pp. 540-543, August 2001.

[26] P. J. Chung, J. F. Bohme and A. O. Hero, "Tracking of multiple moving sources using recursive EM algorithm," *EURASIP Journal on Applied Signal Processing*, vol. 2005, no. 1, pp. 50-60.

[27] P. J. Chung and J. F. Bohme, "DOA estimation of multiple moving sources using recursive EM algorithms," in *Proceedings of IEEE Sensor Array and Multichannel Signal Processing Workshop*, pp. 323-326, August 2002.

[28] L. Frenkel and M. Feder, "Recursive expectation-maximization (EM) algorithms for time-varying parameters with applications to multiple target tracking," *IEEE Transactions on Signal Processing*, vol. 47, no. 2, pp. 306-320, February 1999.

[29] J. C. Chen, K. Yao and R. E. Hudson, "Source Localization and Beamforming," *IEEE Signal Processing Magazine*, pp. 30-39, March 2002.

[30] Y. Huang , J. Benesty and G. W. Elko, "Passive Acoustic Source Localization for Video Camera Steering," *Proceedings of IEEE International Conference on Acoustics, Speech, and Signal Processing*, vol. 2, pp. 909-912, June 2000.

[31] J.A. Bilmes**,** "A gentle tutorial of the EM algorithm and its applications to parameter estimation for Gaussian mixture and hidden Markov models"**,** *Technical Report TR-97-021, International Computer Science Institute, Berkeley, California,* 1998

Vita

Kiran Kumar Mada is from Karimnagar which is in the Southern part of India. He received his Bachelor of Engineering in Electrical and Electronics degree from Osmania University, Hyderabad, in 2003. He enrolled in the Department of Electrical and Computer Engineering at Louisiana State University, Baton Rouge, Louisiana, USA, in the Spring of 2004 and will receive his Master of Science in Electrical Engineering degree majoring in signal processing in Summer 2006.